2nd Regional Conference on Vehicle Engineering and Technology 2008
Kuala Lumpur, 15-17 July 2008

Surge Forces of a FPSO at Lee Side of Submerged Plate in Regular Waves

Agoes Priyanto [a], **Erwandi** [b], **Samudro** [b]

[a] Marine Technology Department, Faculty of Mechanical Engineering
Universiti Teknologi Malaysia, 81310 Skudai Johor Malaysia
[b] Laboratorium Hidrodinamika Indonesia, BPP Teknologi
Kompleks Kampus ITS, Sukolilo Surabaya, 60112 Surabaya Indonesia
agoes@fkm.utm.my

Abstract

A submerged horizontal plate type breakwater is not only to be good energy dissipates of wave breaking on the top of the plate, but also to generate steady flow and to reproduce shorter waves. This paper assessed a submerged plate which is applied to set up for an Oil/Gas Floating Production Storage and Offloading (FPSO) structure. The wave exciting surge forces of the FPSO at the lee side of the submerged plate were examined by using Boundary Element Method based on the potential theory. In order to verify the numerical results, the model experiments have been carried out in Towing Tank of Laboratorium Hidrodinamika Indonesia, BPP Teknologi. By comparing the numerical results with the experimental ones, the results show that the numerical results have similar tendency to the experimental ones, and it is deduced that the submerged plate reduces effectively the wave exciting surge forces at low wave frequencies.

Keywords: submerged plate, wave exciting surge forces, potential theory, floating structure.

1. Introduction

When floating structure terminals in deep water are deployed to serve oil offshore production, storage and offloading, the terminals should withstand their position even in bad weather conditions, and have minimum response motions due to waves. Rubble mound breakwaters are widely used around the world for the construction of artificial harbors and for shore protection works. When sufficient quantity and good quality rubble are not available in the vicinity of the proposed harbor site, then concrete caissons can be used. Both structures cannot be applied to protect a huge floating structure, such as terminal or floating airport in deeper waters. For such conditions, special types of breakwaters, which require less concrete per unit length and are capable of transmitting less wave energy, must be developed. Since in deeper waters most of the wave energy is concentrated near the water surface, a structure is required, which can effectively dissipate or reflect this energy. Immersed horizontal plates were found to be good energy dissipaters due to artificial stimulation of wave breaking on the top of the plates [1]. The horizontal barrier breakwater made from plate structure ("submerged horizontal plate") is can be applied and expected to improve the performance as a breakwater due to the additive properties of wave breaking and reflection. Hence, this type of breakwater is expected to reduce the energy transmission towards the lee side of the structure where the floating terminal on location.

The performance of submerged horizontal plate breakwater type had been studied and given clear results that the submerged plate could make the steady flow and reproduce smaller waves of the incoming waves [2,3,4]. Moreover, Neelamani and Rajendran [5] had reported the hydrodynamic performance of the depth of submergence of the breakwater was varied in order to find out the appropriate depth of immersion at which the wave transmission was minimum, and summarized the results in terms of design curves on submerged plate. These have motivated the authors to investigate the wave transmission, reflection of the submerged plate and wave forces of the terminal at the lee side of the plate. The submerged plate is installed to the floating structure as shown in Fig. 1, and expected to reduce the wave forces and hopefully to minimize the terminal motions in waves.

This paper presents a submerged plate which is applied to set up for a floating structure. The submerged plate parameters, such as the plate's depth of immersion and size, are selected based on the design curves. The appropriately selection the depth of immersion and size of this breakwater is required to achieve the intended wave conditions at the lee side, the present study proved on the characteristics of wave transmission (*Ct*) for a wide range of wave conditions of the selection plate and

compares the *Ct* results with the numerical computer program MEC [6]. One can decide the permissible wave transmission for a particular oil and gas activity at the lee side of the structure after having known the characteristics of incoming waves. For example, for given wave conditions (say peak period of 8 s and significant wave height of 2.0 m), if the permissible transmitted wave height is 0.4 m. The study of energy dissipation character is important to understand the efficiency of the plate as a breakwater. A breakwater can be considered to be performing well if the energy dissipation capability is high. It is also necessary to understand the wave climate at the seaside of the plate due to wave reflection from the breakwater, since the safe navigation of approaching supply vessels is a function of this wave climate. Hence, wave histories are also measured at a typical location at the lee side of the breakwater.

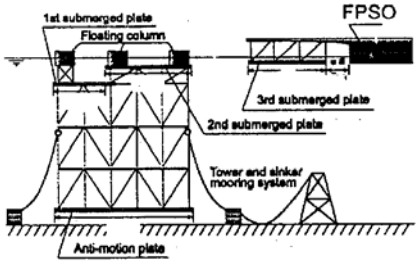

Fig.1. Submerged horizontal plate [4]

Then the hydrodynamic effect of the submerged plate on the wave exciting surge forces are evaluated by boundary element method based on the potential theory. In order to verify the numerical results, the model experiments were carried out in Towing Tank of Laboratorium Hidrodinamika Indonesia, BPP Teknologi.

2. Experimental details

The wave transmission and reflection of the submerged plate, and surge forces of the floating structure at the lee side of the plate were experimentally investigated in a Towing Tank by using physical models. Regular wave is used for the present investigation with the period ranged between 0.8 – 1.24sec and a constant wave height of 0.04m. Details of the experimental investigations are given in this section.

2.1. Wave transmission and reflection of plate

Froude scaling is adopted for physical modeling, which allows for the correct reproduction of gravitational and fluid inertial forces. A scale of 1:50 is chosen for the selection of floating structure and submerged plate model dimensions and wave properties in the present study. Table 1 and 2 give details of the proposed prototype conditions the corresponding model dimensions. The wave transmission and reflection of plate were measured by 3 wave probes (*WP*) on model tests as shown in Fig.2 for a constant water depth of 5.50 m, which corresponds to 275 m water depth in the prototype for 1:50 scale and considers as the deep water depth. *WP1* measured the incident wave, *WP2* measured reflection wave and *WP3* measured the transmission wave.

Tabel 1. Wave conditions

Item	Unit	Prototype	Model
Wave period	sec	5,6 – 10.5	0.8 – 1.49
Wave height	M	2	0.04

Table 2. Main Particulars of submerged plate

Item	Unit	Prototype	Model
Length	M	30	0.6
Thickness	M	1	0.02
Depth of immersion	M	2	0.04

The reflection estimation gives reflection coefficient (*Cr*) as the ratio of reflected and incident wave height (i.e. *Cr*=*Hr*/*Hi*). Similarly, the transmission estimation gives transmission coefficient (*Ct*) as the ratio of transmited and incident wave height. The law of conservation of energy is used for the estimation of the coefficient of energy loss, K_l, since it is not possible to measure it. A breakwater is said to be better if it dissipates most of the incident wave energy. From the law of conservation of energy:

$$C_r^{\,2} + C_t^{\,2} + K_l^{\,2} = 1 \qquad (1)$$

$$K_l = \sqrt{1 - C_r^{\,2} - C_t^{\,2}} \qquad (2)$$

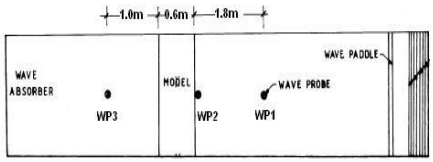

Fig.2. Wave transmission and reflection measurement (*WP1,2,3*)

2.2. Surge forces on floating structure at the lee side of plate

The model is fabricated by using multiplex wood laminated with a fibre sheet. The model

consists of two portions, namely (1) a horizontal plate and (2) a floating production storage offloading (FPSO) pontoon. The size of the horizontal plate is 1.95×0.6×0.02 m3 and the FPSO pontoon is as shown in Table.3. The plate is fixed rigidly in FPSO pontoon's deck by means of frame steel as shown in Fig.3. The frame steel of 50×50×6 mm3 are braced widthwise and lengthwise to ensure strength and rigidity of the plate.

The surge forces at FPSO in wave were measured by a force tranducer fixed at centre of gravity (*CoG*) of the FPSO for two conditions, namely FPSO pontoon only and FPSO with submerged plate. The regular waves were used at model tests, the wave conditions are shown in Table.1.

Table 3. Main Particulars of FPSO model

Item	Unit	Prototype	Model
Length (Lpp)	M	285	5.70
Beam	M	58	1.16
Draught	M	6	0.12
Deck's Height	M	27	0.54
Displacement	ton	89,940	0.701
CoG from keel	m	12.6	0.25
CoG from mid	m	0	0

Fig.3. FPSO with submerged plate model

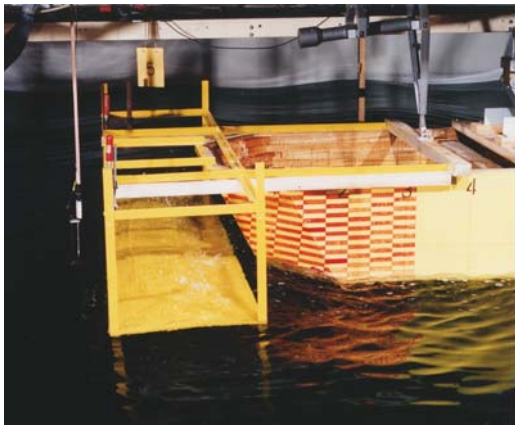

Fig.4. FPSO with submerged plate model in waves

3. Numerical computation

3.1. MEC online computation

The characteristics of wave transmission (*Ct*) for a wide range of wave conditions of the selection plate were compared with the numerical computer program MEC [6]. The MEC computes the performance of the submerged plate in waves by online. The output results from the MEC online computation is visualized through internet. MEC-Online Computation and Online Visualization can be accessed on the following URL:

http://tsumuji2.ga.eng.osaka-u.ac.jp

This homepage is also equipped by the user guide and some simply input files as demonstration version on how to use the MEC program. The user guide and generated file input can be downloaded as illustrated in Fig.5. MEC-Online Computation and Online Visualization consists of three application software:

1. MAST web application server
2. MEC main program (MEC-C) and MEC post-processing program.
3. AVS Express version 6 to visualize the results

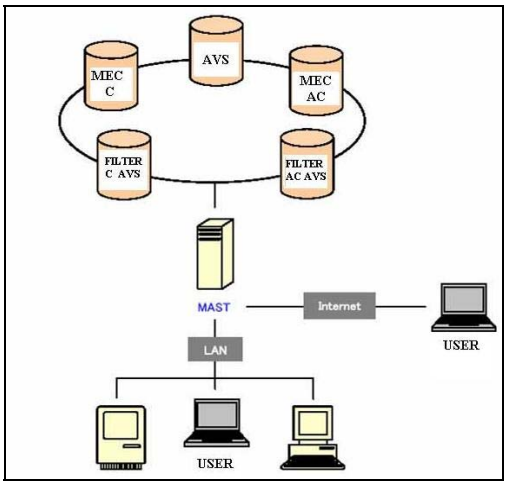

Fig.5. MEC online computation [6]

MAST web application server is the software which has a function to control the interaction among computation programs. The MEC main program is MEC hydrostatic model variable mesh as known as the MEC-C program. AVS Express version 6 is the graphical software that is produced by Advanced Visual System Inc., and visualizes the results from the program Filter C-AVS and Filter AC-AVS.

3.2. Potential Theory

Surge forces, that acts on the FPSO for two conditions (with/without submerged plate) [7], are computed by using 2D boundary element method

based on potential theory and use the coordinate system as shown in Fig.6.

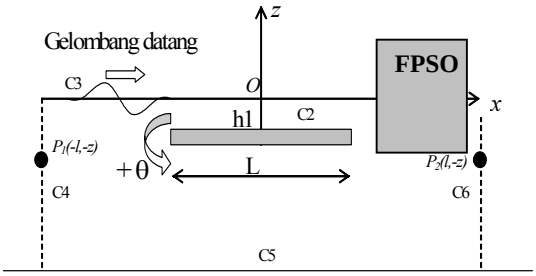

Fig.6. Coordinate system

Two imaginary boundaries are assumed to be located far away from FPSO *x=-l* (boundary *C6*) and *x=l* (boundary *C4*). Since the fluid is inviscid and incompressible, and the flow is irrotational, the velocity potential satisfies the Laplace equation in the whole domain. The velocity potential must also satisfy the following boundary conditions: two imaginary boundaries (*C4,C6*), bottom surface (*C5*), water free surface (*C3*), submerged plate's and FPSO's wetted surfaces (*C1,C2*). By assuming *P* as point in fluid field and *Q* as point in boundary in the Green Formula, so that the radiation boundary value problem (bvp) can be defined as:

$$\alpha\phi_i(P) = \oint_C \frac{\partial\phi_i(Q)}{\partial n}\ln(1/r)ds - \oint_C \phi_i(Q)\frac{\partial}{\partial n}(\ln(1/r))ds \quad (3)$$

where:*C=C1+C2+C3+C4+C5+C6*; the boundaries at the closed domain, *r* is distance between *P* and *Q*, α is radian measure, when *P* is on the boundary *α=π*.

The Eq.(3) can be discretised by dividing the boundary of domain into number of line elements. The velocity potential at an element is expressed in term of its nodal potential value by using linear shape function. The boundaries *C1 – C6* are divided into the number of elements *NE1 – NE6*, respectively. In the numerical computation the numbering of the element on the boundary is in an anticlockwise direction. By substituting the linear shape function into Eq.(3), the discrete bvp is obtained. Let put the boundary conditions into the discrete bvp, the radiation velocity potential at each point hence solved. The surge forces *Ek* in Eq.(4) at FPSO are obtained by applying Haskind Relationship of the incident and radiation velocity potential, and consider the diffraction problem on the wetted surface boundary conditions on FPSO (*C1*).

$$E_k = -i\rho\omega\int_{C2}\left(\phi_0\frac{\partial\phi_k}{\partial n} + \phi_k\frac{\partial\phi_0}{\partial n}\right)ds \quad (4)$$

4. Results and discussion

4.1. Wave transmission and reflection of plate

Figs. 7 and 8 are the output from MEC online computation that show the performance and flow mechanism of the particle waves at full-scale period 7 seconds without and with the submerged plate on location, respectively. The figures show clearly the differences of the vector velocity of the particle wave where the submerged plate is not and on location. The velocity increases on two surfaces' submerged plate and the flow below the plate statrt to return at the end of plate and opposite the direction of the flow on top surface. These two flows make a clash on top surface, and form a steep slope wave.

Fig.8 indicates the wave length at the lee side of the submerged plate is shorter than the incident wave; as well the wave amplitude is smaller.

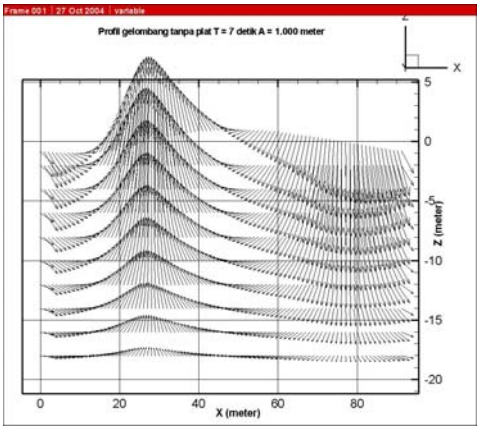

Fig.7. Vector velocity wave particle at T=7sec

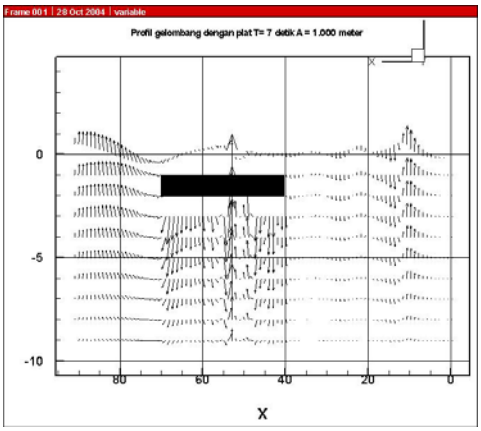

Fig.8. Vector velocity wave particle on submerged plate at T=7sec

Data for each model test run were acquired for a total duration of 30 secs. shown in Fig.9. at a sampling frequency of 50 Hz. Waves were generated for a total duration of 60 s. Depending upon the period of wave generated, data collection

commences 30–65 s after starting the wave generation. This is to make sure that the data collection is started only after repeatability of the same wave heights at the model location is established. The starting time for data collection is set based on trial runs with different periods of waves. The data collection duration is set at 30 s, based on the following criteria:

1. The regular wave time series should have at least 10 wave cycles.
2. The data collection must be completed before any reflected waves, either from the wave maker or from the beach, affect the measurements around the test section.

The tests data were analyzed by using Fourier series method.

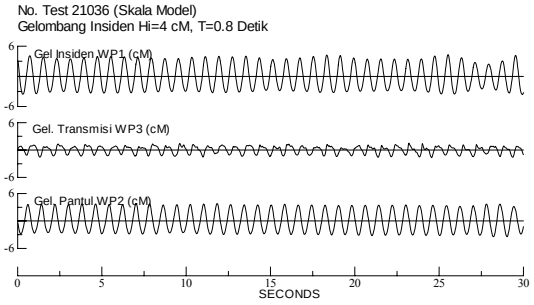

Fig.9. Model tests data at T=0.8s (full-scale T=5.7s) for incident, transmission and reflection wave

Fig.10 show the transmission coefficient *Ct* of the selected plate sizes and it is compared with the MEC online computation. It proves that the average transmission coefficient for the range of period 4 till 12 secs. is about 0.4 as the chosen coefficient in the curve design. From the comparison, the MEC online computation on first component of transmission wave agrees well with the model tests.

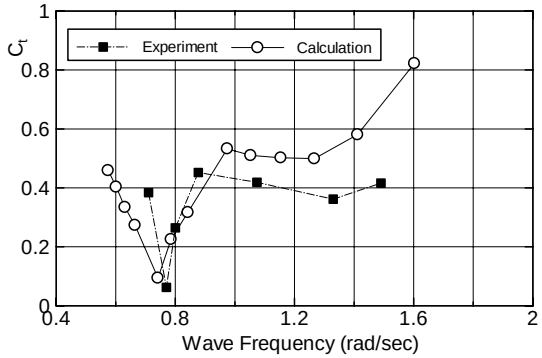

Fig.10. First component in Fourier series of transmission wave

4.2. Surge forces on floating structure at the lee side of plate

The source code of 2D boundary element method was validated to calculate hydrodynamic forces on a square submerged plate in infinite fluid domain. The hydrodynamic forces computation on heave added mass of the square plate is shown in Fig.11, in the same figure the other method is shown for comparison.

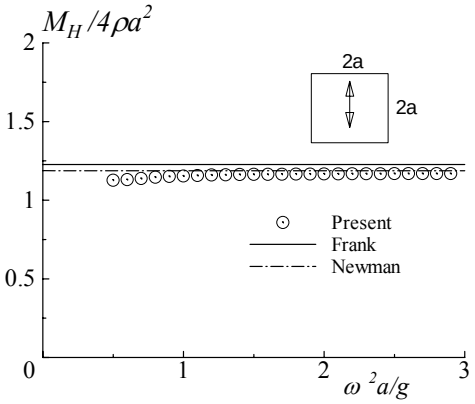

Fig.11. The validation check on 2D BEM code

Fig.12. show the computation on the selected submerged plate with variation effects of the inclination angle on the surge forces Fx . The results are made in nondimensional forces. The figure show that the minimum surge forces on the plate occurs at the angle=0 deg (horizontal plane).

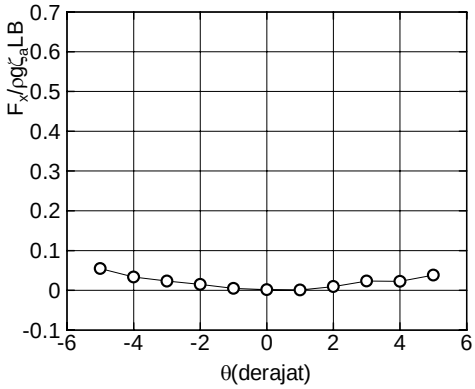

Fig.12. Effect of inclination angle on the surge forces on the plate at period 7 secs.

In model tests to measure the surge forces on the FPSO, Fig.13 show an example of capturing data on wave height and surge forces of FPSO in irregular wave using the Jonswap spectra with Hs=2m and Tp=11secs.

Fig.14 show the surge forces results on FPSO for two conditions, namely freely floating and at the lee side of the submerged plate. The computations using 2D BEM are also shown in the same figure for comparison. The computation results have similar tendency with the model tests both for two conditions. It is found that the surge forces on FPSO at the lee side of the submerged plate reduce at low incident wave below 1 rad/sec. Moreover at high wave frequencies, the surge forces of FPSO are same as the freely floating condition. On the

other word the incident wave does not reduce at the submerged plate.

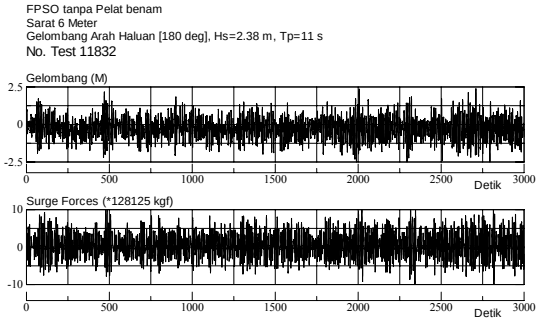

Fig.13. Time histories of surge forces of FPSO in irregular waves.

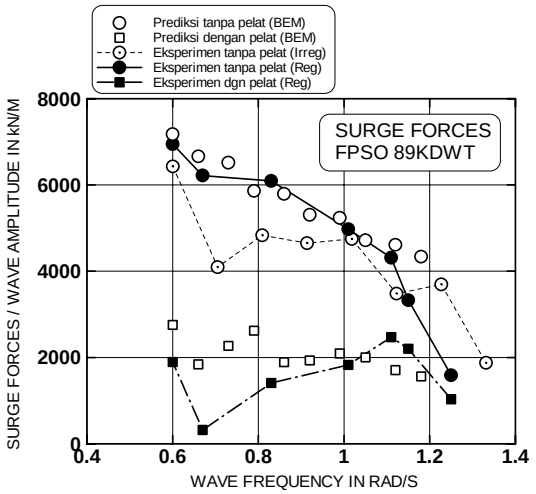

Fig.13. Surge forces of FPSO at the lee side of (with) the submerged plate.

5. Conclusion

When the waves approach the plate, the wave particles flow velocity increase on two surfaces (top and base). The base flow returns at the end of plate and clashes with the top flow, hence it forms a steep slope wave at water surface.

The MEC online computations on the first component transmission wave have agreed well with the model tests. The transmission coefficient for the selected submerged plate is about 0.4 in period range of 4 till 12 secs.

The inclination effect on the surge force of the submerged plate is small. The minimum surge force of the plate occurs at the angle of inclination=0 degree.

The wave exciting surge forces of the FPSO at the lee side of the submerged plate have been examined by using 2D Boundary Element Method based on the potential theory. By comparing the numerical computations with the tests data, the results show that the numerical results have similar tendency to the experimental ones, and it is deduced that the submerged plate reduces effectively the wave exciting surge forces at low wave frequencies.

Acknowledgements

Authors acknowledged the Ministry of Research and Technology of Republic Indonesia for financial supports through RUTXI/2004 research grant.

References

1. Patarapanich, M., Maximum and zero reflection from submerged plate. Journal of the Waterways, Harbors and Coastal Engineering Division 110 (2), 175–181,1984.
2. Takaki, et al., Experimental Study on the Hydrodynamic Forces Acting on a Floating Type Breakwater, Proceedings of 14th Ocean Engineering Symposium, pp.271-278, 1988.
3. Takaki, et al., Experimental Study on Breakwater Performance of a Submerged horisontal Plate, Proceedings of 8th Ocean Engineering Symposium, pp.259-266, 1988.
4. Takaki, et al, Hydrodynamic Characteristics of a Submerged Horisontal Plate, Transactions of the West Japan Society of Naval Architects, No.101, pp. 81-88, 2001.
5. Neelamani, S., Rajendran, R., Wave interaction with T-type breakwaters. Ocean Engineering (Technical Notes), 2000.
6. Erwandi, Toda, Y., Asakura, H., Iwata, Y., and Wayama, T. , The Development of the Online Computation and Online Visualization System of the MEC-Model, Journal Kansai Society N.A. Japan, No.241, pp.211-219, 2004.
7. Priyanto, A, Laporan Akhir Pelaksanaan RUT XI (2006)", Menristek RI, January 2006.

PREDICTION OF ADDED RESISTANCE OF SHIP DUE TO REGULAR HEAD WAVES

M.P Abdul Ghani [a], **J. Julait** [b]

[a] Universiti Teknologi Malaysia
[b] Jurong Shipyard , Singapore
pauzi@fkm.utm.my

Abstract

This paper presents the added resistance of a 100m Product Tanker due to waves. It includes the study of influence of ship speed and wavelength to the added resistance. This work was carried out by theoretical calculation and model testing in towing tank. The method proposed by Gerritsma & Beukelmen was used in the theoretical calculation technique. This method required ship motion and hydrodynamic coefficient data as an input, which was determined using Strip Theory. Meanwhile, the model testing was carried out on a 3.382 m model in the towing tank 120m x 4m x 2.5m at the Universiti Teknologi Malaysia's (UTM) Towing Tank in Skudai, Johore Bahru. Both of the techniques were investigated in three Froude number values, namely 0.21, 0.25 and 0.28. For each Froude number, the study was conducted at wavelength to model length ratio, L_w/L_m between 1.0 and 2.0. The outcomes from both experimental and theoretical calculations were also compared.

Keywords: added resistance; strip theory

1. Introduction

The success of a ship design ultimately depends on its ability to sustain its calm water performance in a seaway. Added resistance in waves is an important part of ship performance due to its economical effect on ship operation.The knowledge of added resistance due to waves and possibility to minimize it by changes in ship particulars and hull form has stirred up the operator's interest in optimizing ships in this respect[3]. Added resistance in waves can be determined from model tests or analytical methods. Model experiments are carried out in regular or irregular head seas, and added resistance is measured as the difference between the time average resistance in waves and the calm-water resistance measured at the same speed

2. Experimental Study

2.1. Model Testing

The resistance tests in calm water and in regular waves were carried out in the towing tank 120m x 4m x 2.5m of Marine Technology Laboratory UTM. This laboratory is equipped with the hydraulic driven and computer controlled wave generator which is capable to generate regular and irregular waves over a period range of 0.5 to 2.5 secs. The irregular waves characterized by JONSWAP or Pierson-Moskowitz spectrum can be generated up to a significant wave height of 0.44m, while it is also possible to generate irregular wave according to a spectrum of an arbitrary form.
For this experimental study a model of a 100m product tanker with 31.93 scale ratio was used. The main particulars of the ship and model as shown in Table 1.

Table 1. Ship and Model Particulars

Item	Ship	Model
Length Overall L_{OA}	108.00	3.382
Length Between Perpendicular	100.00	3.132
Breath B	17.50	0.548
Bow Height h_B	14.37	0.450
Depth D	9.25	0.290
Draught Forward T_f	6.65	0.208
Draught Aft T_a	6.65	0.208
Volume Displacement ∇	8695	0.267
VCG or KG	5.00	0.157
LCG aft of FP	49.05	1.536
Rad. of gyration, 25%L, K_{yy}	25	25
Rad. of gyration, 40%B, K_{xx}	40	40
Block Coefficient, C_B	0.747	0.747
Midship Coefficent, C_M	0.952	0.952

2.2. Calm Water Testing

The calm water experiments were carried out for three model speeds which are 1.0925, 1.2745 and

1.4567 m/s. These speeds are equivalent to 12, 14 and 16 knots of ship speed according to the Froude's Law of Similitude.

2.2. Regular Head Waves Testing

For conventional ship forms, a sufficient number of tests should be carried out at each speed to provide adequate data for a range of wavelength from 0.5 L_{bp} to 2.0 L_{bp} [7]. For this experiment, regular head waves were used covering a wave length to ship length ratio from 1.0 to 2.0. The wave height to ship length is varied for different model speed. The testing protocol for this regular head waves experiment stated in Table 2.

Table 2: Regular waves details used in resistance tests in waves

V_m (m/s)	F_n	Wave characteristics				
		L_w/L_m	L_w (m)	H_w (m)	T_w (s)	ω rad/s
1.093	0.197	1.00	3.13	0.039	1.416	4.436
1.093	0.197	1.10	3.45	0.043	1.486	4.230
1.093	0.197	1.30	4.07	0.051	1.615	3.891
1.093	0.197	1.40	4.39	0.055	1.676	3.750
1.093	0.197	1.50	4.70	0.059	1.735	3.622
1.093	0.197	1.70	5.32	0.067	1.847	3.402
1.093	0.197	2.00	6.26	0.063	2.003	3.137
1.275	0.230	1.20	3.76	0.038	1.552	4.050
1.275	0.230	1.40	4.39	0.044	1.676	3.750
1.275	0.230	1.60	5.01	0.050	1.792	3.507
1.275	0.230	1.80	5.64	0.056	1.900	3.307
1.275	0.230	2.00	6.26	0.063	2.003	3.137
1.457	0.263	1.00	3.13	0.026	1.416	4.436
1.457	0.263	1.20	3.76	0.031	1.552	4.050
1.457	0.263	1.40	4.39	0.037	1.676	3.750
1.457	0.263	1.50	4.70	0.034	1.735	3.622
1.457	0.263	1.60	5.01	0.042	1.792	3.507
1.457	0.263	1.80	5.64	0.040	1.900	3.307

The added resistance in regular waves is the difference between the calm water resistance and the resistance in the waves at the same speed.
The added resistance obtained from the experiment would be presented in the form of the nondimensional resistance coefficient σ_{AW} versus nondimensioanl frequency of encounter, $\omega_e(L/g)^{1/2}$. The nondimensional resistance coefficient is expressed as,

$$\sigma_{AW} = \frac{R_{AW}}{\rho g (B^2/L)\xi^2} \qquad (1)$$

It is seen from the above equation that the assumption about added resistance being proportional to the wave height squared is contained in this nondimensional ratio.

3. Theoretical Approximation

There are several theoretical methods to obtain added resistance of ship in waves. However, based on the study done by Aribas and Strom-Tejsen et .al the Gerritsma and Beukelmen method has been used to predict the added resistance in waves in this study.
This method requires information about the ship hull i.e. the sectional offsets or sectional geometric coefficients as an input.
Hydrodynamic characteristics such as added mass and damping coefficients are also required for the stations that define the ship hull. Calculations are performed for a range of regular waves and the hydrodynamic coefficients must be provided for each wave frequency, and also the heave and pitch motion value. In this work, strip theory was used to determine these inputs.

4. Results and discussion

4.1. Influence of Speed and Wave Length on Added Resistance

Figures 1 and 2 shows the plot of experimental and theoretical non dimensional added resistance against wave length to model length ratio of three different Froude numbers, respectively. Figure 1 shows that the added resistance increases with model speed. The peak value occurred at the ratio wave length to model length of 1.5 to 1.6. Results by theoretical calculation demonstrated that added resistance decreases when model speed is increased before peak value region. But, the added resistance increases at and after the peak value region with increasing model speed. These maximum added resistances occur at wave length to model length ratio around 1.4 to 1.6.

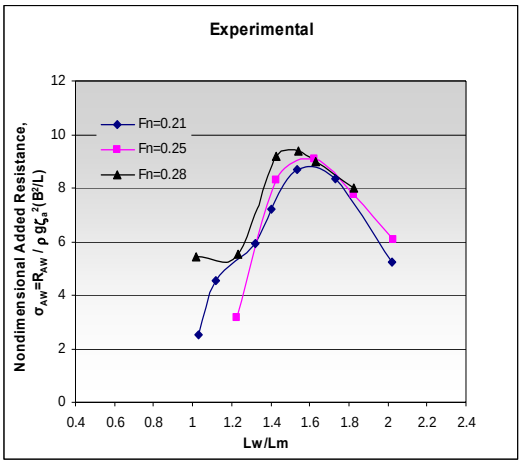

Figure 1: Experimental NonDimensional Added Resistance

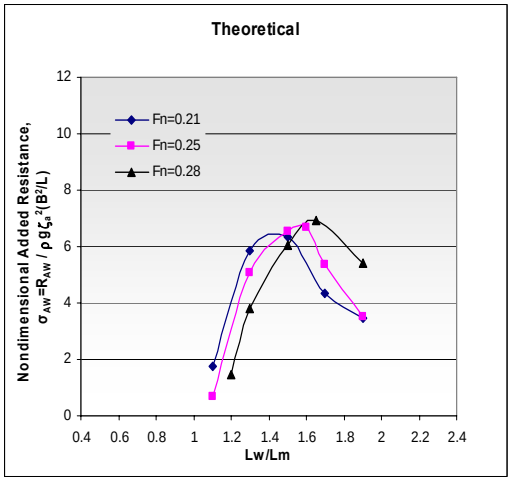

Figure 2: Theoretical NonDimensional Added Resistance

3.2. Comparison of Experimental and Theoretical Added Resistance Results

Figures 3, 4 and 5 illustrate non dimensional added resistance versus wave length to model length ratio, L_w/L_m at Froude numbers 0.21, 0.25 and 0.28, respectively. The peak value of both experimental and theoretical results for F_n=0.21 occurred at approximately 1.5 of L_w/L_m. Meanwhile, the maximum value was observed at 1.6 of L_w/L_m for F_n=0.25. However, in F_n=0.28, the maximum value of experimental data and theoretical data occurred at different L_w/L_m. The peak value of experimental data seems to have occurred at 1.5 of L_w/L_m while the theoretical data was at 1.6.

Generally, the added resistance values obtained in experimental testing were seems higher than the theoretical calculation. However, the differences of value at lower L_w/L_m (high frequencies) was smaller than at higher L_w/L_m. It was supported by the theory that at high frequencies, the diffraction effect constitute the major portion of the added resistance and the Gerritsma and Beukelman's method have included this effects [6]. Thus, it may conveniently be concluded that at lower L_w/L_m the theoretical was to be in closer agreement with the experimental data. Nevertheless, at F_n=0.28, the added resistance of experimental data demonstrated unexpected value at 1.0 of L_w/L_m. This probably due to an experimental error involved during data measurement.

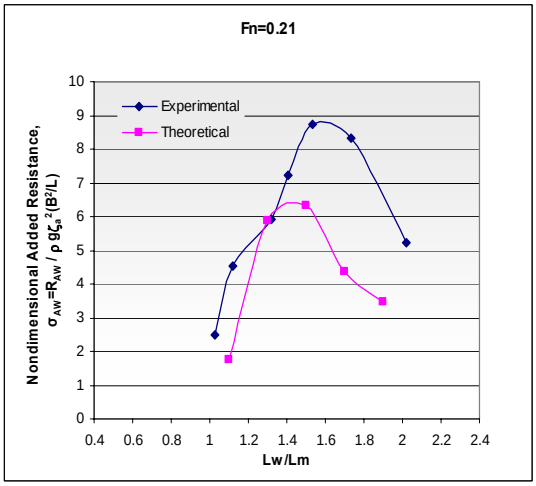

Figure 3: Experimental and Theoretical Added Resistance at Fn = 0.21

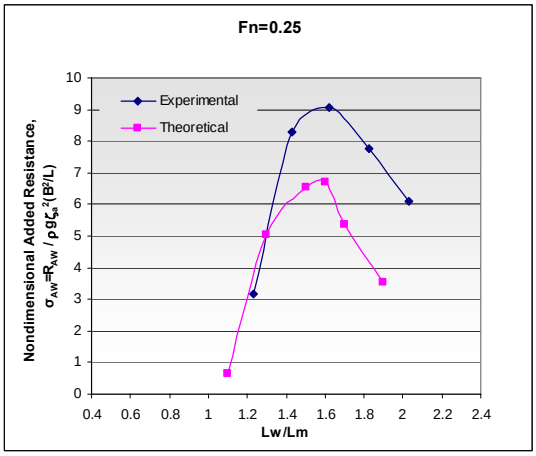

Figure 4: Experimental and Theoretical Added Resistance at Fn = 0.25

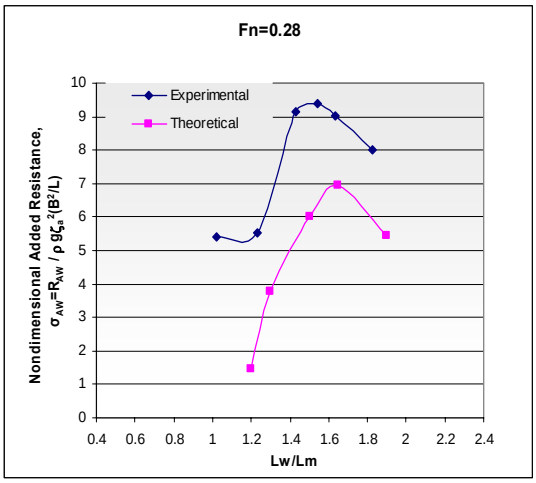

Figure 5: Experimental and Theoretical Added Resistance at Fn = 0.28

It was seen that, in the region of the peak added resistances, the experimental result was approximately 34 % higher than the theoretical result for F_n = 0.21, 34 % for F_n= 0.25 and 33 % for F_n= 0.28. It can be concluded that, at the region of maximum added resistance, the experimental result is approximately 33 % higher than theoretical calculation.

In theoretical calculation, strip theory is a method to determine the ship motion and damping coefficient. The discrepancy between the calculated and measured values may be attributed to these three shortcomings of the strip theory [4].

First, the three-dimensional flow, especially at both ends of the ship, is neglected. The three-dimensional effect on the total damping force, which may not be considered to be large, may cause some discrepancy.

Second, only wave effects have been considered in the calculation of the damping coefficient; damping due to viscosity is neglected in the calculations by the strip theory. Damping due to viscosity in the heaving motion is insignificant only at zero speed.

Third, three-dimensional effects for the calculation of added mass and added mass moment of inertia may also contribute to some extent to the discrepancy between the calculated and measured results.

Another factor that influences the discrepancy between the calculated and measured results is the calculation of the relative motion has a strong effect on the Gerritsma and Beukelman's method. In practice, the presence of hull causes a considerable distortion on the waves close the ship and Equation (29) is only an approximation likely to be reliable at the forward part of the ship. Further aft, the equation may underestimate the relative motion [5]

Data in Table 4.1 summarizes the published data on the region of maximum added resistance. Meanwhile, Table 4 summarizes the differences between experimental and theoretical calculation using Gerritsma and Beukelman's method at the peak value region. The result of this study differs with the other reported study probably because it was conducted under different conditions.

Table 3**:** Peak value region of added resistance

Researcher	**Model**	**Peak value**	**F_n**
Blok, J.J., (1993) [3]	Tanker	1.0 L_w/L_m	0.20
Journee, J.M.J., [6]	Cargo Ship	1.0 L_w/L_m	0.20
MARIN [8]	Tanker	1.2 L_w/L_m	0.20
UTM, (2007)[5]	Tanker	1.5 L_w/L_m	0.21

Table 4**:** Difference between experimental and theoretical (Gerritsma and Beukelman's method)

Researcher	**Model**	**% Diffrence**
Journee, J.M (1976) [6]	Cargo Ship	22 %
Strom-Tejsen (1973) [2]	Series 60 C_B=0.7	25 %
Arribas, F.P., (2006) [1]	Ferry	33 %
UTM, (2007)[5]	Tanker	34 %

5. Conclusion

The added resistance due to waves was increasing when the ship speed was increased. At a certain ship speed, it was increasing due to the increment of wave length. However, after a peak value, the added resistance would decrease. The peak value occurred approximately at 1.5 of wave length to ship length ratio. This is well agreed with the results from the towing tank model testing and theoretical calculation using Gerritsma and Beukelman's method. The result from experimental has shown to be higher than the theoretical calculation. At the peak value region, the differences between experimental and theoretical was approximately 34 %.

Acknowledgements

The authors would like to thank the Marine Technology Laboratory technicians for their assistance in conducting the model tests.

References

1. Aribas, F.P, Some methods to obtain the Added Resistance of a ship Advancing in Waves. Journal of Ocean Engineering, 2006
2. Strom-Tejsen, J., et al, Added Resistance in Waves., Transaction of the SNAME 1973, Vol 81: 109-143.
3. Blok, J.J, The Resistance Increase of a Ship in Waves. Grafisch Bedrijf Ponsen & Looijen BV., Wagenigen 1993

4 Bhattacharyya, R., Dynamics of Marine Vehicles, A Wiley- Interscience Publication, New York, 1978

5. Julait, J, Added Resistance of Ship due to Regular Head Waves, Master Dissertation, Universiti Teknologi Malaysia, Johor Bahru 2007
6. Journee, JMJ, Motion, Resistance and Propulsion of ship in Regular Head Waves, Delf University of Technology, Report 0428, 1976
7. Recommended Procedures and Guidelines, International Towing Tank Conference (ITTC). *Testing and Extrapolation Methods Loads and Responses, Seakeeping Experiments* 7.5-0207-02.1. , 2005
8. MARIN, Model Tests for a Tanker in Irregular and Regular Waves (Model 7698), 1996
9. Harvald. SV.AA. Resistance and Propulsion of Ship. A Wiley- Interscience Publication, New York, 1983